Local redesign for additive manufacturability of compliant mechanisms using topology optimization

Koppen, Stijn; Hoes, Emma; Langelaar, Matthijs; Frecker, Mary I.

Citation (APA)
Koppen, S., Hoes, E., Langelaar, M., & Frecker, M. I. (2021). Local redesign for additive manufacturability of compliant mechanisms using topology optimization. In *ASME 2021 International Design Engineering Technical Conferences and Computers and Information in Engineering Conference : 45th Mechanisms and Robotics Conference (MR)* (Vol. 8A). Article V08AT08A002 ASME. https://doi.org/10.1115/DETC2021-67642

Important note
To cite this publication, please use the final published version (if applicable).
Please check the document version above.

IDETC-CIE 2021

LOCAL REDESIGN FOR ADDITIVE MANUFACTURABILITY OF COMPLIANT MECHANISMS USING TOPOLOGY OPTIMIZATION

Stijn Koppen[*]
Emma Hoes
Matthijs Langelaar
Precision and Microsystems Engineering (PME)
Mechanical, Maritime and Materials Engineering (3ME)
Delft University of Technology (TU Delft)
Delft, South-Holland, 2628 CD
The Netherlands
Email: s.koppen@tudelft.nl

Mary I. Frecker
Department of Mechanical Engineering
Penn State University
University Park, PA USA

ABSTRACT

Compliant mechanisms are crucial components in current and future high-precision applications. Topology optimization and additive manufacturing offer freedom to design complex compliant mechanisms that were impossible to realize using conventional manufacturing. Design for additive manufacturing constraints, such as the maximum overhang angle and minimum feature size, tend to drastically decrease the performance of topology optimized compliant mechanisms. It is observed that, among others, design for additive manufacturing constraints are only dominant in the flexure regions. Flexures are most sensitive to manufacturing errors, experience the highest stress levels and removal of support material carries the highest risk of failure. It is crucial to impose these constraints on the flexure regions, while in others part of the compliant mechanism design, these constraints can be relaxed. We propose to first design the global compliant mechanism layout in the full domain without imposing any design for additive manufacturing constraints. Subsequently we redesign selected refined local redesign domains with design for additive manufacturing constraints, whilst simultaneously considering the mechanism performance. The method is applied to a single-input-multi-output compliant mechanism case study, limiting the maximum overhang angle, introducing manufacturing robustness and limiting the maximum stress levels of a selected refined redesign domain. The high resolution local redesigns are detailed and accurate, without a large additional computational effort or decrease in mechanism performance. Thereto, the method proves widely applicable, computationally efficient and effective in its purpose.

INTRODUCTION

Compliant mechanisms (CMs) achieve force, motion or energy transmission through elastic deformation. Due to their intrinsic high repeatability CMs are crucial components in current and future high-precision applications, among others [1]. In addition to their transmission function, common CM design requirements include range of motion, volume and/or mass, crosstalk and parasitic motion, stress levels and fatigue life as well as the sensitivity of those factors to, *e.g.*, manufacturing errors [1].

CMs are traditionally synthesized by kinematic or building block approaches [2, 3]. The use of Topology Optimization (TO) techniques to design CMs has recently gained increasing interest. TO provides maximum design freedom to create optimal mechanisms satisfying application-specific conflicting requirements whilst requiring minimal designer input regarding mechanism kinematics [4–9].

---

[*]Address all correspondence to this author.

Alongside the increasing popularity of TO, Additive Manufacturing (AM) shows promise as the go-to technology for realization of CMs—particularly that of complex topology optimized CMs [10–12]. The constructive freedom that AM offers allows fabrication of CM designs that were impossible to realize using conventional manufacturing. But also AM capabilities have their limits, which has resulted in the development of specific Design for AM (DfAM) methodologies [13].

The majority of DfAM restrictions are a consequence of the intrinsic layer-wise and temperature intensive nature of AM processes [14, 15]. The most dominant DfAM constraints are the maximum overhang angle and minimum feature size [15]. Furthermore, the kinematic behaviour of CMs is highly sensitive to geometrical deviations arising from manufacturing errors. Additionally, limiting peak stress levels is important for any CM to prevent failure. At the design stage, this requires accurate Finite Element (FE) modeling.

Much attention has been devoted to incorporating DfAM constraints in the TO process, including overhang angle (self-supporting structures) filters/constraints [11, 16–21] as well as support structures [22–24] and (combined) building orientation [23] optimization. Both robustness of performance with respect to uniform AM errors and feature size control can be achieved using the robust TO formulation [25–29]. Inclusion of stress constraints in the TO process of CMs has also been reported [29–32].

However, global DfAM constraints may drastically decrease the performance of CMs designed using TO [11]. In addition, accurate FE modeling requires fine meshes, which—although increasing both design space and modeling accuracy—drastically increase the required computational effort, especially when used within an iterative process such as TO.

Both from analysis and experiments it is observed that DfAM constraints—when applied to lumped CMs—are (only) dominant in the most flexible regions, hereafter simply called flexures. The kinematic behaviour of these flexures is most sensitive[1] to manufacturing errors. In addition, flexures are generally the regions experiencing high stress levels. As opposed to other regions of the design, removal of support material in flexures regions carries high risk of damaging flexures with obvious negative effects. Hence, it is crucial to ensure flexure regions are self-supporting, while in other parts of the CM design, this AM constraint can be relaxed.

To address these challenges, we propose a two-step CM TO method:

(i) first design the global CM layout in the full domain (using TO) <u>without</u> DfAM considerations, and subsequently
(ii) redesign selected refined local redesign domain(s) (flexures) <u>with</u> DfAM considerations, whilst simultaneously considering the mechanism performance.

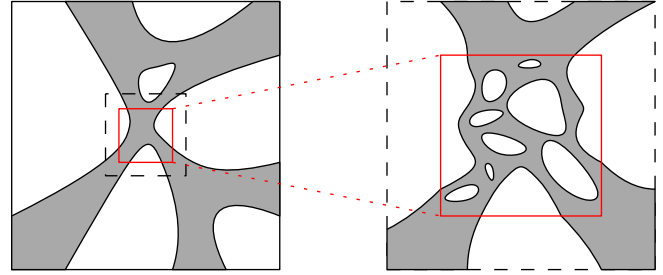[1]Bending stiffness scales cubically with thickness.

FIGURE 1: A two-step approach towards DfAM using TO.

Fig. 1 shows a schematic representation of the proposed idea. The topology of the global design on the left is analyzed and a selection of local redesign domain(s) is made. The right schematic shows the topology of the high-resolution flexure redesign—possibly taking into account DfAM constraints. An additional advantage of the proposed method is that through employing static condensation, as detailed in the next section, the second refined design stage has low computational cost while still accounting for the performance of the entire mechanism.

In general, a global design may have multiple redesign domains that should be reconsidered simultaneously. For simplicity and without loss of generality, we consider a single redesign domain throughout the remainder of the present work. We also assume that the designer manually selects the redesign region(s). As an extension these could be identified automatically using geometrical and strain-based indicators.

The manual post-processing method of Shih et al. [33] allows for local redesign, however it does not facilitate the use of topology optimization nor the local application of constraints. The method proposed in this work has—to the best knowledge of the authors—not been explored yet.

The expected advantages of this approach are twofold, namely:

(i) detail and accuracy where it matters, with low additional computational effort, and
(ii) DfAM where it is required, without drastically decreasing the mechanism performance.

Hereafter the method is further outlined. This is followed by implementation details, after which we apply the method to a case study with different DfAM and performance constraints.

METHOD

The method consists of three subsequent phases, visualized in Fig. 2:

(i) Generation of the global CM design—possibly via TO—without taking into account DfAM constraints. This generally is an iterative process.
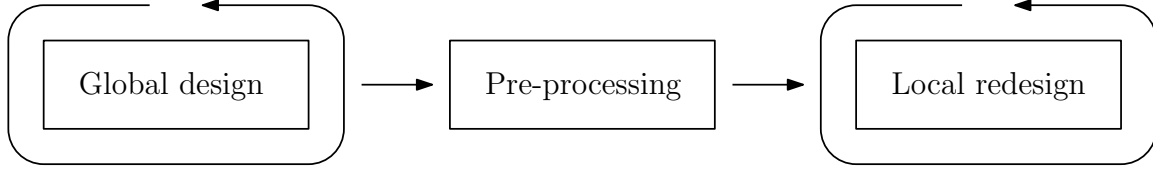
FIGURE 2: Flowchart of the three subsequent phases required to locally redesign for AM of CMs using TO.

(ii) Pre-processing of the redesign phase including stiffness mapping and mesh coupling.

(iii) Redesign of the local domain(s) using TO taking into account DfAM constraints. Similar to the global design phase, this is an iterative process.

Whereas the first phase relies on established state-of-the-art, both the pre-processing and local redesign phases require further explanation. In what follows, both phases are further elaborated.

Pre-processing

The pre-processing phase subsequently consists of

(i) definition of local redesign domain(s),

(ii) partitioning of structural Degrees of Freedom (DOFs) in three disjoint sets: non-design, interface and redesign,

(iii) mapping of the non-design domain stiffness to the interface DOFs,

(iv) re-initialization of the local redesign domain(s) (with refined mesh),

(v) coupling of non-matching meshes between the interface and redesign domain(s), and

(vi) adjustment of filters (density and/or overhang) to take into account non-design topology within filter radius.

Consider a global design as visualized on the left of Fig. 1. After locating the local redesign domain(s), in this case the flexure, we split up the structural DOFs of the discretized partial differential equation in three sets, consecutively containing the DOFs in the redesign domain (○), non-design domain (●) and interface (■) regions, as visualized in Fig. 3. Some redesign DOFs (●) are coupled to the interface DOFs to ensure mesh continuity.

Since only a small part of the structure is subject to change, the computational effort can be significantly reduced if the dimensionality of the problem is reduced before the redesign phase, such that repetitive analysis of the non-design domain(s) is avoided. We propose to a priori apply exact model-order reduction in the form of static condensation to map the stiffness of the non-design domain to the interface without loss of information [34–38]. In addition, this highly reduces the computational effort of the sensitivity analysis [39]. To this end, consider the discretized governing system of equations $\mathbf{Bu} = \mathbf{f}$, partitioned in
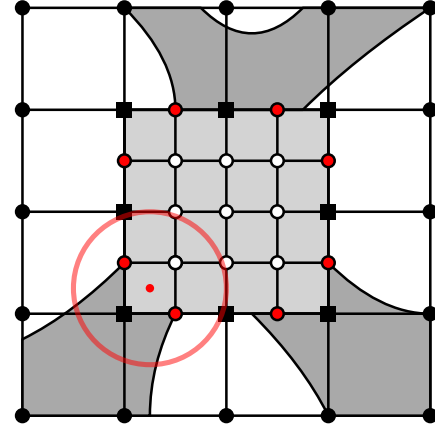

FIGURE 3: Reinitialization of redesign domain. The structural DOFs are separated in three sets, the DOFs in the redesign domain (○), non-design domain (●) and interface (■) regions. Some redesign DOFs (●) are coupled to the interface DOFs using MPCs. Note that for some design variables the filter radius (both for density and overhang filter) exceeds outside of the redesign domain, as indicated by the red circle.

DOF sets of the interface (i) and non-design (n) domain, *i.e.*

$$\begin{bmatrix} \mathbf{B}_{ii} & \mathbf{B}_{in} \\ \mathbf{B}_{ni} & \mathbf{B}_{nn} \end{bmatrix} \begin{bmatrix} \mathbf{u}_i \\ \mathbf{u}_n \end{bmatrix} = \begin{bmatrix} \mathbf{f}_i \\ \mathbf{f}_n \end{bmatrix}. \tag{1}$$

Via the condensation process we obtain the reduced system of discretized governing equations, solely in terms of the interface DOFs, *i.e.*

$$\tilde{\mathbf{K}}\mathbf{u}_i = \mathbf{f}_i + \tilde{\mathbf{f}}, \tag{2}$$

with the reduced system matrix

$$\tilde{\mathbf{K}} := \mathbf{B}_{ii} - \mathbf{B}_{in}\mathbf{B}_{nn}^{-1}\mathbf{B}_{ni}, \tag{3}$$

and the reduced load

$$\tilde{\mathbf{f}} := -\mathbf{B}_{in}\mathbf{B}_{nn}^{-1}\mathbf{f}_n. \tag{4}$$

3

Here we assume the principal sub-matrix $\mathbf{B}_{nn}$ to be non-singular, such that it is invertible [40]. Note that the preconditioning of the—generally high dimensional—matrix $\mathbf{B}_{nn}$ can be reused. The reduced system matrix and load are independent of the design variables. Thereto, this—relatively expensive—process only needs to be carried out once prior to the redesign.

Note that the interface DOFs generally are the geometrical interface between non-design and redesign domain, however may also include other DOFs, for example the DOFs at input/output of a mechanism. By doing so, one does not have to recompute the displacement field of condensed DOFs via the displacement field of the interface DOFs via

$$\mathbf{u}_n = \mathbf{B}_{nn}^{-1}\left(\mathbf{f}_n - \mathbf{B}_{ni}\mathbf{u}_i\right). \tag{5}$$

Note that $\mathbf{B}_{nn}^{-1}\mathbf{f}_n$ has previously been calculated in Eq. (4). Without loss of generality, in the remainder of the present work we assume all relevant DOFs are included as interface DOFs, including the DOFs with applied loads. As a result, we assume $\tilde{\mathbf{f}} = \mathbf{0}$.

After mapping of the non-design domain stiffness, the local redesign domain is remeshed with a finer mesh and reinitialized. The mesh of the redesign domain is non-conforming with respect to the interface mesh (Fig. 3). To circumvent discontinuities in the displacement field, mesh coupling is required to enforce continuity. One can introduce weak geometric compatibility via Multi-Point Constraint (MPC) methods such as, *e.g.*, main-secondary elimination, penalty function augmentation or Lagrange multiplier adjunction [41]. Without loss of generality we opt to linearly couple the interfacing redesign DOFs (●) to adjacent interface DOFs (■) via the main-secondary elimination technique. Consider the uncoupled discretized governing system of equations $\mathbf{A}\left[\mathbf{x}\right]\mathbf{u} = \mathbf{f}$, partitioned in DOF sets of the interface (i) and redesign (r) domain. The design-dependent stiffness matrix $\mathbf{A}\left[\mathbf{x}\right]$ has not yet been assembled with the non-design domain stiffness $\tilde{\mathbf{K}}$. A transformation matrix $\mathbf{T}$ is constructed[2], coupling the dependent redesign DOFs to the interface DOFs via

$$\mathbf{u} = \mathbf{T}\mathbf{v}, \tag{6}$$

with $\mathbf{v}$ the independent main DOFs. Thereto, after premultiplication of the discretized system of equations by $\mathbf{T}^{\mathsf{T}}$, the constrained stiffness matrix is simply calculated via

$$\mathbf{K}\left[\mathbf{x}\right] = \mathbf{T}^{\mathsf{T}}\mathbf{A}\left[\mathbf{x}\right]\mathbf{T}. \tag{7}$$

The mesh refinement also influences any filtering techniques used in the TO process, *e.g.* the common density filter [42] or

---

[2]This is considered common knowledge and hence not elaborated.

overhang filter [11]. As shown in Fig. 3, if the filter radius exceeds the interface, the filter operator has to be adapted to include the non-design topology in order to ensure a smooth transition between the redesign and non-design domains. In the present work, this is simply handled by refining the density description in these boundary regions of non-design elements.

Local redesign

After pre-processing one can rewrite the original optimization problem formulation, in terms of the redesign variables and DOFs, *i.e.*

$$\begin{aligned} \underset{\mathbf{x}}{\text{minimize}} \quad & g_0\left[\mathbf{x}, \mathbf{v}\left[\mathbf{x}\right]\right] \\ \text{subject to} \quad & g_i\left[\mathbf{x}, \mathbf{v}\left[\mathbf{x}\right]\right] \leq 0, \quad i = 1, ..., m \\ & x_i \in \mathbb{X}, \quad\quad\quad i = 1, ..., N \end{aligned} \tag{8}$$

with $\mathbf{x} \in \mathbb{R}^N$ the design variables, each satisfying the bound constraints, that is $\mathbb{X} := \{x \in \mathbb{R} \mid 0 \leq x \leq 1\}$, $g_0\left[\mathbf{x}, \mathbf{v}\left[\mathbf{x}\right]\right]$ the objective function as used for the global CM design, now written in terms of the displacement field of the redesign and/or interface $\mathbf{v}\left[\mathbf{x}\right]$, and $g_i\left[\mathbf{x}, \mathbf{v}\left[\mathbf{x}\right]\right]$ the CM and/or DfAM constraints imposed on the redesign domain.

To solve the optimization problem in Eq. (8), we follow—with the exception of some small adaptations—the standard procedure for "density based sequential approximate TO" [7]. This entails iteratively performing the following steps until convergence:

(i) Density filter (and possibly AM and/or Heaviside filter)
(ii) Material interpolation
(iii) Redesign stiffness matrix assembly
(iv) Coupling of redesign and interface meshes using MPCs
(v) Assembly of redesign and non-design domain stiffnesses
(vi) Finite element analysis
(vii) Response evaluation and sensitivity analysis
(viii) Optimization of convexified subproblem

The adjustment of filter and transformation operators have been explained in the pre-processing phase. The largest deviation from the standard process is step (v): assembly of redesign and non-design domain stiffnesses.

In order to incorporate the full structural behaviour into the redesign process, the reduced system matrix $\tilde{\mathbf{K}}$ is combined with the constrained stiffness matrix $\mathbf{K}\left[\mathbf{x}\right]$ and load properties of the redesign domain via

$$\begin{bmatrix} \mathbf{K}_{rr}\left[\mathbf{x}\right] & \mathbf{K}_{ri}\left[\mathbf{x}\right] \\ \mathbf{K}_{ir}\left[\mathbf{x}\right] & \mathbf{K}_{ii}\left[\mathbf{x}\right] + \tilde{\mathbf{K}} \end{bmatrix} \mathbf{v} = \mathbf{T}^{\mathsf{T}} \begin{bmatrix} \mathbf{f}_r \\ \mathbf{f}_i \end{bmatrix}. \tag{9}$$

The low dimensional discretized governing equations of Eq. (9) can now be used to analyze the structural response at a highly

reduced computational effort. As such, it is relatively cost effective to carry out redesign at specifically chosen local domains. Since the reduced stiffness matrix is design-independent, it does not influence the sensitivity analysis, which is omitted here for brevity.

IMPLEMENTATION

Independent of the problem formulation as presented, the user has to consider, select, and implement a variety of methods to effectively use the formulation in a topology optimization setting. Without loss of generality, the case study employs the implementation choices described here.

For the finite element analysis, we opt for standard 4-node quadrilateral (2D) elements in structured meshes. The domain is parametrized by assignment of a design variable $x_i \in \mathbb{X}$ to each finite element i, which allows for local control of the material properties [7].

It is generally recognized that both final topology and performance are sensitive to the initial design. This is especially the case for CM TO. We consider this influence out of the scope of this paper and thereto opt for a homogeneous initial design, both for the global design and local redesign. The volume fraction of the local redesign initial design is set equal to the volume fraction of the redesign domain of the global design.

To eliminate modeling artifacts, the design variable field $\mathbf{x}$ is generally blurred as to obtain the filtered field $\tilde{\mathbf{x}} \in \mathbb{R}^N$ using a linear filtering operation with radius $r \in \mathbb{R}^+$, see *e.g.* [42]. The modification of filter operator has further been explained under pre-processing.

The Young's modulus of an element is related to the filtered design variable $\tilde{x}_i$ via an element-wise composite rule. We apply the commonly used modified solid isotropic material with penalization interpolation function [6], that is

$$E_i[\tilde{x}_i] = \underline{E} + \left(\overline{E} - \underline{E}\right)\tilde{x}_i^p, \tag{10}$$

with $\underline{E}$ and $\overline{E}$ the Young's moduli of void and solid and $p \in \mathbb{R}^+$ a user definable parameter. It is known that this interpolation function stimulates a 0/1 solution of a compliance-based optimization problem with volume constraint.

The gradient-based inequality-constrained nonlinear optimization problem in Eq. (8) is solved in a nested analysis and design setting. The design variables are iteratively updated by a sequential approximate optimization scheme, as is common in the topology optimization field. We use the method of moving asymptotes by Svanberg [43], including the parameter settings provided therein. The resulting convex sub-problems are solved using a primal-dual interior point method. The optimization is terminated when the maximum design change is smaller than a termination value.

CASE STUDY

To illustrate the effectiveness and versatility of the proposed method, it is applied to a case study, based on the single-input-multi-output CM design example used in [7]. Consider the global design problem posed in Fig. 4a and corresponding optimization problem formulation

$$
\begin{aligned}
&\underset{\mathbf{x}}{\text{maximize}} && g_0\left[\mathbf{v}\left[\mathbf{x}\right]\right] := u\left[\mathbf{x}\right] \\
&\text{subject to} && \frac{w^2\left[\mathbf{x}\right]}{u^2\left[\mathbf{x}\right]} \leq \overline{\varepsilon} \\
& && V\left[\mathbf{x}\right] \leq \overline{V} \\
& && x_i \in \mathbb{X}, \quad i = 1,...,N
\end{aligned}
\tag{11}
$$

with $u[\mathbf{x}]$ the output displacement, $w[\mathbf{x}]$ the parasitic motion, $\overline{\varepsilon}$ the maximum allowable relative displacement, $V[\mathbf{x}]$ the volume fraction of the redesign and $\overline{V}$ the maximum allowable volume fraction (set to 0.2 for the global design problem). The objective is to maximize the output displacement u, while constraining the parasitic motion w both due to an imposed unit load f at the input. The topology of the global design obtained by solving Eq. (11), with parameters set as given in Table 1 is shown in Fig. 4b. The volume fraction of the redesign domain is $\tilde{V}$. The remaining redesigns are subjected to $\overline{V} = \tilde{V}$ for fair comparison. The applied refinement factors for each redesign case are listed in Table 2.

The reference redesign, that is the redesigned flexure without additional refinement or constraints, is shown in Fig. 5a and we define its reference performance as $g_0 = \tilde{g} = 1$ (normalized output displacement). The refined (6 times) redesign is shown in Fig. 5d and has performance $g_0 = 1.03\tilde{g}$. The increased design space allows for minor improved performance.

In the following we will show the possibilities of introducing additional DfAM or performance constraints: limiting the maximum allowable overhang angle, introducing manufacturing robustness, or limiting the maximum stress levels in the formulation as posed in Eq. (11), without providing a thorough investigation of design parameters.

Self-supporting flexure

This variation includes a simplified AM fabrication model to exclude unprintable geometries from the design space, resulting in fully self-supporting (maximum 45° overhang angle) optimized designs [11]. The problem formulation as posed in Eq. (11) is unaltered. However, the TO process includes an additional filtering step between the density filter and material interpolation. The resulting topologies corresponding to a north and west building direction are shown in Figs. 5b and 5c, respectively. A redesign with north building direction can easily be obtained without any loss of performance ($g_0 = 1.00\tilde{g}$), see
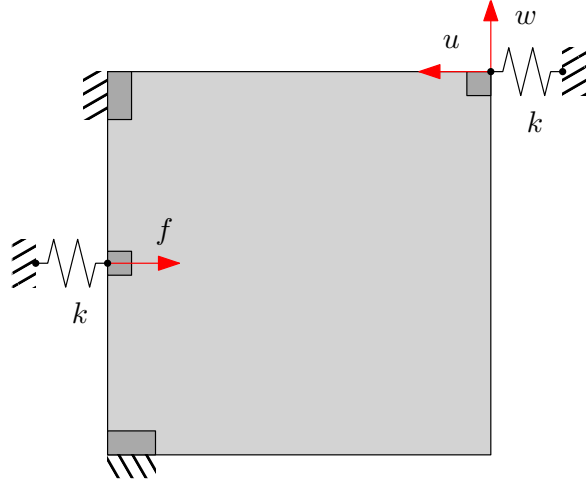
(a) Design domain and boundary conditions. The domain is discretized in 80 by 80 square quadrilateral finite elements.
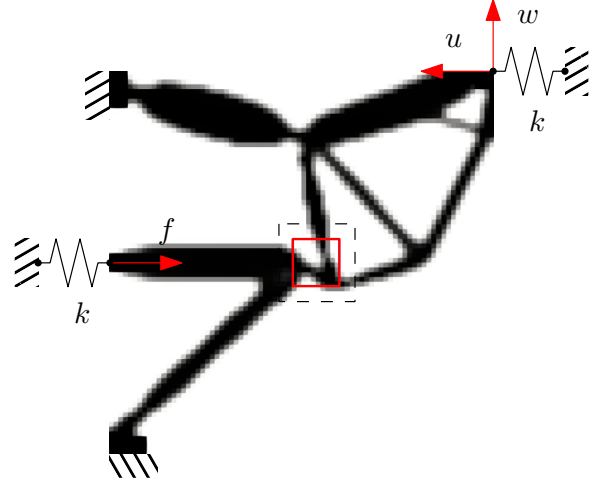
(b) Topology resulting from solving Eq. (11).

FIGURE 4: Single-input-multi-output CM design problem.

TABLE 1: Case study constant parameters

Parameter	Value	Description
$\overline{E}$	1.0 Pa	solid Young's modulus
$\underline{E}$	1.0×10^{-9} Pa	void Young's modulus
r	2.0	filter radius (no. of elements)
p	3.0	SIMP penalty
k	0.1 N m^{-1}	actuator stiffness
$\overline{\varepsilon}$	0.01	relative crosstalk

the results summarized in Table 2. However, the topology of the west building direction highly deviates from the reference and a loss of performance is observed ($g_0 = 0.87\tilde{g}$).

Whilst these redesigned domains are self-supporting, the remainder of the design is not (per se). When including the overhang filter on the full design domain, no feasible solutions are found for any of the four building directions (south, east, north, west). These solutions do not satisfy the constraints and/or the design variables take on intermediate values.

Stress-optimized flexure

In order to limit the maximum stress for a given range of motion, or similarly extend the range of motion for a given maximum stress, one can extend the problem formulation in Eq. (11)

with stress constraints, *i.e.*

$$g_{\sigma} := \max\left(\boldsymbol{\sigma}\left[\mathbf{x}\right]\right) \leq \overline{\sigma}, \tag{12}$$

with $\boldsymbol{\sigma}$ the stress field, for example using the Von Mises stress criterion, and $\overline{\sigma}$ the maximum allowable stress. Many different formulations of g_{σ} are available, see *e.g.* [29,31,32] for CM specific formulations. Without loss of generality, we use the unified aggregation and relaxation approach as proposed by Verbart et al. [44].

Figure 5e depicts the stress constrained redesign. Here $\overline{\sigma}$ is set to 0.3 times the maximum stress of the topology as obtained in Fig. 5d. Despite the strict constraint, the topology has a similar performance to the refined redesign; see Table 2.

If the problem formulation includes stress constraints on the full design domain, a performance reduction of at least 15% is observed.

Robust flexure

The desired kinematics and stress field of a flexure is sensitive to geometric deviations. However, in classical deterministic topology optimization, the effect of such uncertain parameters on the performance of the structure is not taken into account. This may lead to a design that is very sensitive to manufacturing errors. As a consequence, the performance of the actual structure may be far from optimal.

The robust approach to topology optimization [25,26,28,45] takes into account uniform manufacturing errors. Uniform erosion and dilation effects, from here on denoted by superscripts (e) and (d), are simulated by means of a projection method: the
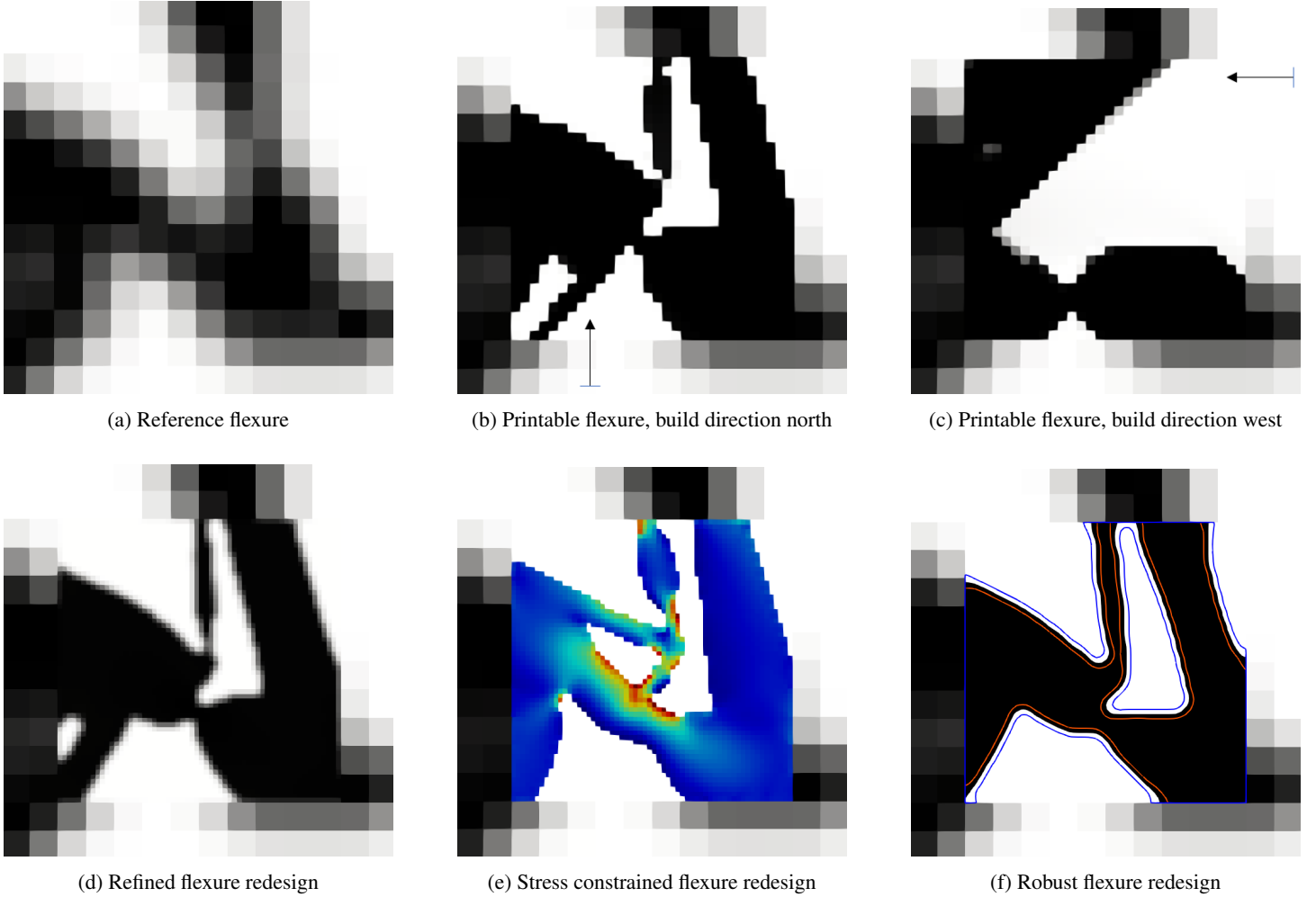
(a) Reference flexure

(b) Printable flexure, build direction north

(c) Printable flexure, build direction west

(d) Refined flexure redesign

(e) Stress constrained flexure redesign

(f) Robust flexure redesign

FIGURE 5: A variety of refined redesigned flexures with varying refinement ratios and DfAM constraints.

filtering of the design variable field is followed by a differentiable Heaviside projection using a high projection threshold η^{e} to simulate an erosion and a low projection threshold η^{d} to simulate a dilation. For further details on the robust formulation the reader is referred to [26].

Considering the robustness one can reformulate the problem formulation in Eq. (11) as

$$
\begin{aligned}
\underset{\mathbf{x}}{\text{maximize}} \quad & g_0\left[\mathbf{v}\left[\mathbf{x}\right]\right] := \min\left(u\left[\mathbf{x}^{\mathrm{e}}\right], u\left[\mathbf{x}^{\mathrm{d}}\right]\right) \\
\text{subject to} \quad & \frac{w^2\left[\mathbf{x}^i\right]}{u^2\left[\mathbf{x}^i\right]} \leq \bar{\varepsilon}, \quad i \in \{\mathrm{e},\mathrm{d}\} \\
& v\left[\mathbf{x}^{\mathrm{d}}\right] \leq \bar{v} \\
& x_i \in \mathbb{X}, \quad i = 1,\ldots,N
\end{aligned}
\tag{13}
$$

Note the objective function now is a "max-min" formulation be-

tween the output displacement of eroded and dilated topologies. The constraint on parasitic motion is applied to both the eroded and dilated topologies, whereas the volume constraint is applied to the worst-performing field, that is the dilated topology.

The resulting flexure topology is shown in Fig. 5f. Here the blue and red contours indicate the dilated and eroded geometry boundaries, respectively. It is observed that the robustness requirement has a large impact on performance, see Table 2. However, apart from the robustness, one guarantees both a minimum feature size on solid and void. In addition and opposed to foregoing results, the robust formulation also provides perfect 0/1 solutions, which lowers the probability of performance decrease upon design interpretation (*e.g.* post-processing conversion to CAD model).

7

TABLE 2: Case study results

Result	g_0	Refinement	Comment
Fig. 5a	1.00	1	Reference
Fig. 5b	1.00	3	Overhang filter (north)
Fig. 5c	0.87	3	Overhang filter (west)
Fig. 5d	1.03	6	Refined
Fig. 5e	1.03	6	Stress constrained
Fig. 5f	0.80	6	Robust

CONCLUSIONS

The combination of topology optimization and additive manufacturing has great potential for compliant mechanism design. However, global design for additive manufacturing constraints have a large impact on both topology and performance. As found in the present work, for some cases, a feasible solution is unreachable or even non-existent. Therefore, instead of global design, a two-step local redesign approach is proposed, targeting performance-critical flexure regions. While performing a local redesign, the method is nevertheless based on performance evaluations of the entire mechanism.

The computational effort of the proposed local redesign method is relatively small as compared to the global design phase. For 3D problems, the computational efficiency of the method is expected to increase further. The exact additional effort depends on the number, size and refinement ratios of local design domains.

The presented compliant mechanism case study demonstrates the possibility to locally control printability, stress or robustness. The simultaneous consideration of these constraints as well as the extension of the method to 3D are directions for future work.

Although applied to CM design with DfAM constraints, the generality of the method allows application to any problem in which constraints are locally dominant.

The method allows to apply constraints locally, at those regions it matters most, without drastically decreasing the global performance. In addition, the high resolution local redesign domains are detailed and accurate, without a large additional computational effort. Thereto, the method proves versatile, computationally efficient and overall effective.

REFERENCES

[1] Howell, L. L., 2001. *Compliant Mechanisms*. John Wiley & Sons, Ltd., New York.

[2] Gallego, J. A., and Herder, J., 2009. "Synthesis methods in compliant mechanisms: An overview". *Proc. ASME Des. Eng. Tech. Conf.,* **7**, pp. 193–214.

[3] Danun, A. N., Palma, P. D., Klahn, C., and Meboldt, M., 2021. "Building block synthesis of self-supported three-dimensional compliant elements for metallic additive manufacturing". *Journal of Mechanical Design,* **143**(5).

[4] Larsen, U., Sigmund, O., and Bouwstra, S., 1997. "Design and fabrication of compliant micromechanisms and structures with negative Poisson's ratio". *Journal of Microelectromechanical Systems,* **6**(2), jun, pp. 99–106.

[5] Frecker, M. I., Ananthasuresh, G. K., Nishiwaki, S., Kikuchi, N., and Kota, S., 1997. "Topological Synthesis of Compliant Mechanisms Using Multi-Criteria Optimization". *Journal of Mechanical Design, Transactions of the ASME,* **119**(2), jun, p. 238.

[6] Sigmund, O., and Torquato, S., 1997. "Design of materials with extreme thermal expansion using a three-phase topology optimization method". *Journal of the Mechanics and Physics of Solids,* **45**(6), pp. 1037–1067.

[7] Bendsøe, M. P., and Sigmund, O., 2004. *Topology Optimization*. Springer Berlin Heidelberg.

[8] Deepak, S. R., Dinesh, M., Sahu, D. K., and Ananthasuresh, G. K., 2009. "A Comparative Study of the Formulations and Benchmark Problems for the Topology Optimization of Compliant Mechanisms". *Journal of Mechanisms and Robotics,* **1**(1), feb, p. 011003.

[9] Cao, L., Dolovich, A. T., and Zhang, W. J., 2013. "On understanding of design problem formulation for compliant mechanisms through topology optimization". *Mechanical Sciences,* **4**(2), pp. 357–369.

[10] Mirth, J. A., 2016. "The design and prototyping of complex compliant mechanisms via multi-material additive manufacturing techniques". In International Design Engineering Technical Conferences and Computers and Information in Engineering Conference, Vol. 50152, American Society of Mechanical Engineers, p. V05AT07A003.

[11] Langelaar, M., 2016. "Topology optimization of 3D self-supporting support structures for additive manufacturing". *Additive Manufacturing,* **21**, pp. 666–682.

[12] Khurana, J., Hanks, B., and Frecker, M., 2018. "Design for additive manufacturing of cellular compliant mechanism using thermal history feedback". In International Design Engineering Technical Conferences and Computers and Information in Engineering Conference, Vol. 51753, American Society of Mechanical Engineers, p. V02AT03A035.

[13] Rosen, D., 2014. "Design for additive manufacturing: past, present, and future directions". *Journal of Mechanical Design,* **136**(9).

[14] Gao, W., Zhang, Y., Ramanujan, D., Ramani, K., Chen, Y., Williams, C. B., Wang, C. C., Shin, Y. C., Zhang, S., and Zavattieri, P. D., 2015. "The status, challenges, and future of additive manufacturing in engineering". *Computer-*

Aided Design, 69, pp. 65–89.

[15] Diegel, O., Nordin, A., and Motte, D., 2019. *A Practical Guide to Design for Additive Manufacturing*. Springer.

[16] Gaynor, A. T., and Guest, J. K., 2016. "Topology optimization considering overhang constraints: Eliminating sacrificial support material in additive manufacturing through design". *Structural and Multidisciplinary Optimization, 54*(5), pp. 1157–1172.

[17] Langelaar, M., 2017. "An additive manufacturing filter for topology optimization of print-ready designs". *Structural and multidisciplinary optimization, 55*(3), pp. 871–883.

[18] van de Ven, E., Maas, R., Ayas, C., Langelaar, M., and van Keulen, F., 2018. "Continuous front propagation-based overhang control for topology optimization with additive manufacturing". *Structural and Multidisciplinary Optimization, 57*(5), pp. 2075–2091.

[19] Garaigordobil, A., Ansola, R., Veguería, E., and Fernandez, I., 2019. "Overhang constraint for topology optimization of self-supported compliant mechanisms considering additive manufacturing". *CAD Computer Aided Design, 109*, apr, pp. 33–48.

[20] Pellens, J., Lombaert, G., Lazarov, B., and Schevenels, M., 2019. "Combined length scale and overhang angle control in minimum compliance topology optimization for additive manufacturing". *Structural and Multidisciplinary Optimization, 59*(6), pp. 2005–2022.

[21] van de Ven, E., Maas, R., Ayas, C., Langelaar, M., and van Keulen, F., 2020. "Overhang control based on front propagation in 3d topology optimization for additive manufacturing". *Computer Methods in Applied Mechanics and Engineering, 369*, p. 113169.

[22] Kuo, Y.-H., Cheng, C.-C., Lin, Y.-S., and San, C.-H., 2018. "Support structure design in additive manufacturing based on topology optimization". *Structural and Multidisciplinary Optimization, 57*(1), pp. 183–195.

[23] Langelaar, M., 2018. "Combined optimization of part topology, support structure layout and build orientation for additive manufacturing". *Structural and Multidisciplinary Optimization, 57*(5), pp. 1985–2004.

[24] van de Ven, E., Ayas, C., Langelaar, M., Maas, R., and van Keulen, F. "Accessibility of support structures in topology optimization for additive manufacturing". *International Journal for Numerical Methods in Engineering*.

[25] Sigmund, O., 2009. "Manufacturing tolerant topology optimization". *Acta Mech. Sin. Xuebao, 25*(2), pp. 227–239.

[26] Wang, F., Lazarov, B., and Sigmund, O., 2011. "On projection methods, convergence and robust formulations in topology optimization". *Struct. Multidiscip. Optim., 43*(6), pp. 767–784.

[27] Schevenels, M., Lazarov, B. S., and Sigmund, O., 2011. "Robust topology optimization accounting for spatially varying manufacturing errors". *Computer Methods in Applied Mechanics and Engineering, 200*(49-52), dec, pp. 3613–3627.

[28] Lazarov, B. S., Schevenels, M., and Sigmund, O., 2011. "Robust design of large-displacement compliant mechanisms". *Mechanical Sciences, 2*(2), aug, pp. 175–182.

[29] da Silva, G. A., Beck, A. T., and Sigmund, O., 2019. "Topology optimization of compliant mechanisms with stress constraints and manufacturing error robustness". *Computer Methods in Applied Mechanics and Engineering*, jun.

[30] Saxena, A., and Ananthasuresh, G. K., 2001. "Topology optimization of compliant mechanisms with strength considerations*". *Mechanics of Structures and Machines, 29*(2), pp. 199–221.

[31] de Leon, D. M., Alexandersen, J., Fonseca, J. S. O., and Sigmund, O., 2015. "Stress-constrained topology optimization for compliant mechanism design". *Structural and Multidisciplinary Optimization, 52*(5), nov, pp. 929–943.

[32] de Assis Pereira, A., and Cardoso, E. L., 2018. "On the influence of local and global stress constraint and filtering radius on the design of hinge-free compliant mechanisms". *Structural and Multidisciplinary Optimization, 58*(2), pp. 641–655.

[33] Shih, C. J., Lin, C. F., and Chen, H. Y., 2006. "An integrated design of flexure hinges and topology optimization for monolithic compliant mechanism". *Journal of Integrated Design and Process Science, 10*(3), jan, pp. 1–16.

[34] Guyan, R., 1965. "Reduction of stiffness and mass matrices". *AIAA J., 3*(2), pp. 380–380.

[35] Irons, B., 1965. "Structural eigenvalue problems - elimination of unwanted variables". *AIAA J., 3*(5), may, pp. 961–962.

[36] Botkin, M., and Yang, R., 1989. "Three-Dimensional Shape Optimization with Substructuring". *AIAA J., 29*(3), pp. 486–488.

[37] Gangadharan, S., Haftka, R., and Nikolaidis, E., 1990. "Easily implemented static condensation method for structural sensitivity analysis". *Commun. Appl. Numer. Methods, 6*(3), apr, pp. 161–171.

[38] Yang, R., and Lu, C., 1996. "Topology Optimization with Superelements". *AIAA J., 34*(7), pp. 1533–1535.

[39] Koppen, S., Langelaar, M., and van Keulen, F., 2021. "Efficient multi-partition topology optimization". *Computer Methods in Applied Mechanics and Engineering, **TO BE PUBLISHED***.

[40] Benscoter, S., 1948. "The partitioning of matrices in structural analysis". *J. Appl. Mech., 15*(4), pp. 303–307.

[41] de Boer, A., van Zuijlen, A. H., and Bijl, H., 2007. "Review of coupling methods for non-matching meshes". *Computer methods in applied mechanics and engineering, 196*(8), pp. 1515–1525.

[42] Bruns, T., and Tortorelli, D., 2001. "Topology optimiza-

tion of non-linear elastic structures and compliant mechanisms". *Comput. Methods Appl. Mech. Eng., **190***(26-27), pp. 3443–3459.

[43] Svanberg, K., 1987. "The method of moving asymptotes—a new method for structural optimization". *International Journal for Numerical Methods in Engineering, **24***(2), feb, pp. 359–373.

[44] Verbart, A., Langelaar, M., and van Keulen, F., 2017. "A unified aggregation and relaxation approach for stress-constrained topology optimization". *Struct. Multidiscip. Optim., **55***(2), feb, pp. 663–679.

[45] da Silva, G. A., Cardoso, E. L., and Beck, A. T., 2020. "Comparison of robust, reliability-based and non-probabilistic topology optimization under uncertain loads and stress constraints". *Probabilistic Engineering Mechanics*, feb, p. 103039.